

Vadym Zhukovskiy, Oleksandr Gokhman, Marianna Kondrya
South Ukrainian National Pedagogical University named after K. D. Ushynsky, Odesa, Ukraine

STUDY OF SURFACE MICROSTRAINS BY ELECTRON SPECKLE-INTERFEROMETRY METHODS

Received: June 05, 2017 / Revised: June 24, 2017 / Accepted: June 26, 2017

© Zhukovskiy V., Gokhman O., Kondrya M., 2017

Abstract. Despite the fact that speckle interferometry methods began to develop more than 30 years ago, they still remain a rather exotic laboratory tool that has not received wide practical application in tensometry measurements and flaw detection. There are two reasons. The first one is the problem to interpret the interferograms by the right way. The second one is the extremely low measurement speed, which makes it impossible to use these methods for study of fast processes.

In this paper we propose the advanced algorithm for electronic speckle interferometry (ESPI) method, which uses the arctangent of the intensity ratio of the speckles of two quarter-phase shifted specklograms, from that the position of the surface points with a known time step is calculated. Summing the increments of displacements after each measurement, we obtain a picture of the distribution of the strains of the surface of the object under study in the 3-dimensional representation customary for the experimenter. This approach effectively solves the first mentioned problem.

While considering the second problem, it is shown that the measurement speed can be raised to the speed of the camera used (up to 1000 measurements per second in the flesh) if at the calibration stage a pair of speckles on the spectrograph is determined, whose phase is shifted by a quarter, and then take the arctangent of their ratio Intensities.

In this case, there is no need to displace the reference beam, and the calculation of the displacement of the surface is made entirely from one specklogram only. Despite the fact that in this case the resolving power of the method bit decreases, the measurement speed increases substantially and there is no effect of the dynamic characteristics of the elements of the reference arm of the speckle interferometer on the measurement result, which is especially important in high-speed photography.

The suggested algorithm for ESPI provides the extension of the diapason of recorded microstrains to hundreds of microns as well as on-line observation in 3D mode. New perspectives of nanoscale technologies could be opened on this way.

Keywords: speckle interferometry, tensometry measurements, space distribution of strains.

Introduction

Electronic Speckle Pattern Imaging (ESPI) method is well-known method to receive the distribution of microstrains on surface, which appear due special disturbed tests [1]. The main advantage of EPSI method in comparison with local tensometry methods [2] is a high accuracy to study in-situ the space field on constructions.

The resolving power (d) of the ESPI method is determined by the sensitivity of the pixel of the camera to the change in speckle intensity:

$$d = 0.5I / N ,$$

where, I is the wavelength of the laser; N is the resolution of the ADC matrix (usually 255). From the given above equation, d of the ESPI is about 1 nm for purpura colour, which is approximately 10,000 times more accurate than in the method of videography [3].

Nevertheless, the application of ESPI method is episodic. The reason is a relatively low speed, and, consequently, high requirements for vibration stability during measurements. In this paper, algorithms are proposed for the analytical calculation of the position of points on the surface, which make it possible to immediately generate a 3-dimensional representation of the distribution of strains.

This approach has a fundamental difference from the methods of correlation speckle interferometry [4; 5], where the result is a 2-dimensional picture of the correlation bands of speckle phases, and the problem of reconstructing a 3D image has a rather non-trivial solution.

Theoretical basis of the two-frame method of EPSI

In the case of coherent illumination of randomly inhomogeneous objects, such as a rough surface or a transparent medium with a refractive index fluctuating in space, a speckle structure (an interference pattern formed by diffuse scattered light) is formed in the scattered field [5], an enlarged fragment of which is represented in Fig. 1.

For the speckle field, a spatial distribution of intensities is characteristic, which is capable of interfering with a coherent (spherical, plane) or the same speckle-modulated wave. The result of the interference is a speckle field too, where the redistribution of intensities occurs. To describe the principle of the proposed ESI method, consider a single speckle model. As such a model, we use the interference pattern of two plane waves in a Michelson interferometer (Fig. 2).



Fig. 1. Speckle pattern in the field of diffraction of a laser beam on a rough surface

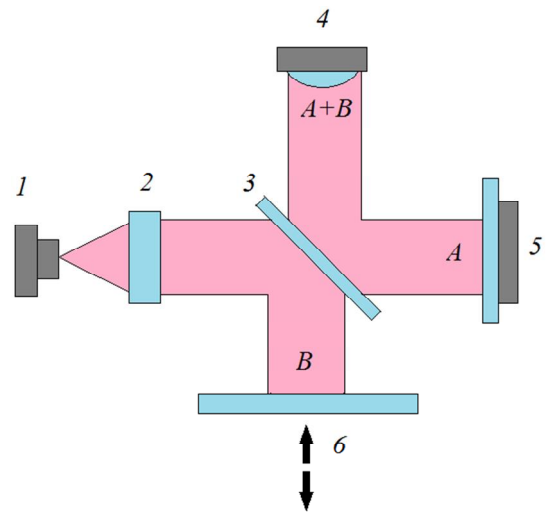


Fig. 2. Michelson's interferometer, which simulates the feedback of one speckle to displacement:
1 – laser diode; 2 – collimator; 3 – beam divider, 4 – photodiode; 5 – mirror on piezoceramics; 6 – normally moving mirror

The result of interference of two waves with intensity I_A and I_B will be a wave whose intensity I_{A+B} changed along the shoulder B by harmonic law (Fig. 3):

$$I_{A+B} = I_A + I_B + 2\sqrt{I_A I_B} \cos k\Delta, \quad (1)$$

where Δ is the difference between the arms of the interferometer (A and B); $k = 2\pi / \lambda$.

If we add a small increment to shoulder A using piezoceramics (5) $\lambda / 4$, the phase will change to $\pi / 2$ and the intensity I_{A+B} will vary according to the law of the sine:

$$I_{A+B} = I_A + I_B + 2\sqrt{I_A I_B} \cos\left(k\Delta - \frac{\pi}{2}\right) = I_A + I_B + 2\sqrt{I_A I_B} \sin k\Delta. \quad (2)$$

In order that the model does not depend on the method of measuring the intensity, we introduce a function normalizing from -1 to 1:

$$F = 2 \cdot \frac{I_{\max} - I_{A+B}}{I_{\max} - I_{\min}} - 1, \quad (3)$$

where I_{\max} and I_{\min} are the maximum and minimum values that the intensity I_{A+B} assumes when moving along the arm of the interferometer. The graphs of the function F for the cases (1) and (2) are shown in Fig. 3. Let us note that the graph of equation (2) will be ahead of or behind the schedule (1) (Fig.

3) depending on the increase or decrease Δ . Thus, these two graphs carry the information about the direction of the displacement.

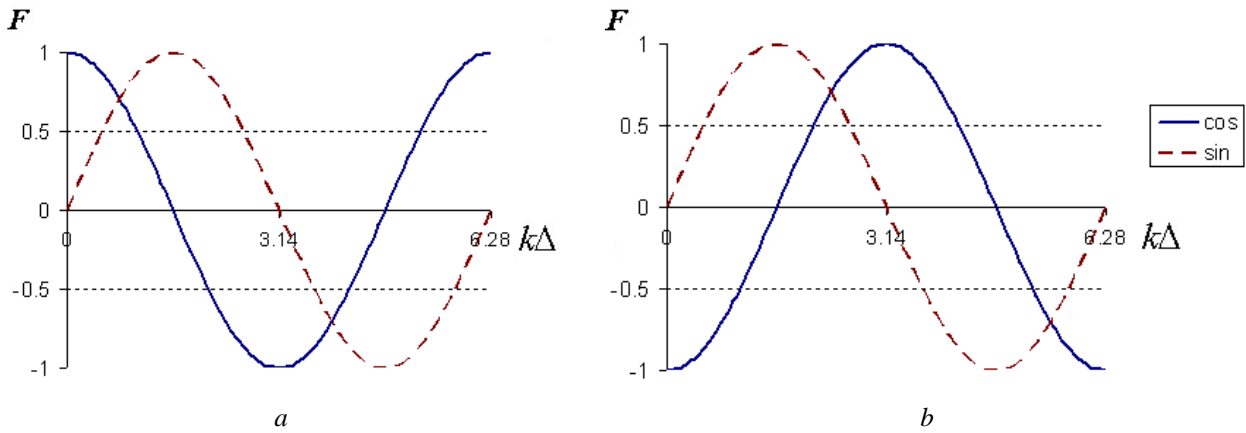


Fig. 3. The change of the normalized intensity of speckle when moving along the arm of the interferometer: *a* – when moving upwards; *b* – when moving downwards

Let F_1 is the normalized intensity without increment of the phase, and F_2 is a the normalized intensity with phase increment $p/2$. The phase diagram $F_1(F_2)$ has the form of a circle with rotation counter-clockwise for the movement is “up” and clockwise for the movement is “down” (Fig. 4) [6].

At the point M_i , the phase can be determined from the relation: $k\Delta = \arctan(F_1 / F_2)$.

In order to avoid the uncertainty when dividing by zero, it is advisable to use a function $\arctan 2(F_1, F_2)$, that is commonly used in programming languages, for example C++:

$$k\Delta = \arctan 2(F_1, F_2) = 1/2 \left[i \ln \left(\frac{i + F_1 / F_2}{i - F_1 / F_2} \right) \right], \quad (4)$$

where i is the imaginary unit.

The function $\arctan 2(F_1, F_2)$ is periodic and has a discontinuity at the point $p/2$ (Fig. 5).

We introduce a certain increment of the phase (dm_i) equal to the phase difference between the points M_{i-1} and M_i :

$$dm_i = M_{i-1} - M_i = \arctan 2(F_1, F_2)_{i-1} - \arctan 2(F_1, F_2)_i. \quad (5)$$

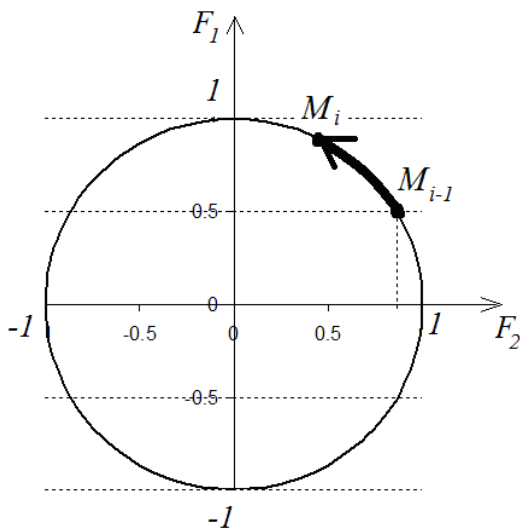


Fig. 4. The phase diagram

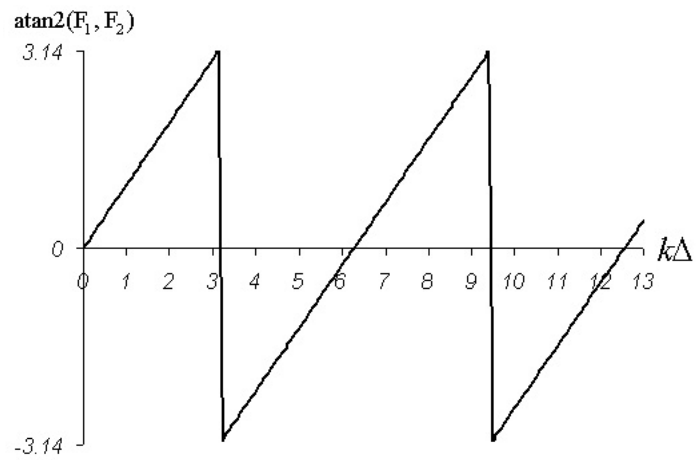


Fig. 5. Function $\arctan 2(F_1, F_2)$

According to (5), the phase difference $k\Delta$ can be written as a sum of increments dm_i :

$$k\Delta = \sum_{i=1}^n dm_i, \begin{cases} \text{if } (dm_i^2 < p^2) \\ \{k\Delta = k\Delta + dm_i;\} \\ \text{else} \\ \{k\Delta = k\Delta + 0;\} \end{cases} \quad (6)$$

Then the function $\arctan 2(F_1, F_2)$ turns into a continuous function phase dependence on the displacement (Fig. 6).

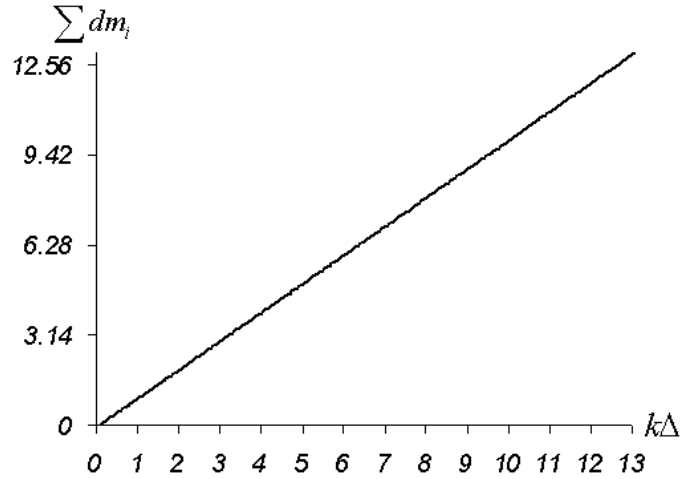


Fig. 6. The plot of the dependence of the sum of the phase increment on the displacement

Due to the discontinuity in the time delay point between the registrations, there should be less than twice the oscillation period of the function F , which corresponds to Kotel'nikov's theorem according to which, in order to reconstruct the graphs of the function F (see Fig. 3) should be more than twice as high as the oscillation frequency of the function F .

Let us note that the interference wave is standing in our study. Hence, its wavelength l is equal to half the wavelength $l/2$ of the radiation of the laser.

Taking into account all the material given above, let us write down the equation for determining the displacement along the arm of the interferometer in terms of the intensity of one speckle:

$$\Delta = \frac{l}{4p} \sum_{i=1}^n dm_i, \begin{cases} \text{if } (dm_i^2 < p^2) \\ \{\Delta = \Delta + dm_i;\} \\ \text{else} \\ \{\Delta = \Delta + 0;\} \end{cases} \quad (7)$$

To obtain the field of displacements along the surface, equation (7) must be applied to each speckle on a specklogram (Fig. 1).

Example of experimental application

In this paper, the proposed two-frame ESPI method has been used to study the stress-strain state of a composite-cement and epoxy resin filled steel reinforcement (Fig.7).

As a testing disturbance, the sample was heated centrally at 5 °C. As a result of this effect, the inhomogeneous parts of the sample perceive the thermal load differently, which is manifested in its inhomogeneous distribution of strains.

In Fig. 8 shows the ESPI encoder circuit. A distinctive feature of the proposed scheme is that it interferes with speckle fields created on a piezoceramic washer (5), a rough surface (6) (diffusely reflecting plate) and diffusely reflecting the surface of the sample (7). The interference result of the two speckle fields will also be a speckle field, which is recorded by the CCD camera (4).

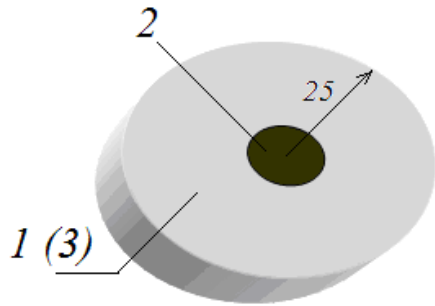


Fig. 7. Models of structural cells of concrete:
1 – cement stone; 2 – fittings; 3 – epoxy resin

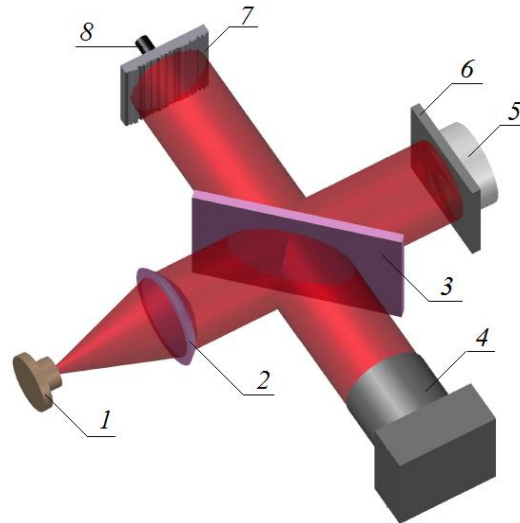


Fig. 8. Schematic of the ESI encoder:
1 – laser diode; 2 – collimator; 3 – beam divider;
4 – CCD camera; 5 – piezoceramic washer;
6 – diffusely reflecting plate; 7 – sample; 8 – heater

The measurement process using the ESI encoder can be divided into three stages: calibration; obtaining of primary data; data processing and image formation.

The first step is to determine the voltage that must be applied to the piezoceramic (5) to ensure a phase shift on $p / 2$. To do this, a speckle is selected arbitrarily on the specklogram recorded by the camera (4) and the voltages at which it has the minimum and maximum intensity are fixed. The difference in these voltages divided by two into the piezoceramic will, in the future, ensure a phase shift of the interfering fields on $p / 2$. Then, a measurement is made, followed by recording in separate arrays, the minimum and maximum intensity of each individual speckle. These data are subsequently used in the intensity normalization according to Eq. (3).

At the second stage, a test disturbance is activated and a series of pairs of images with a phase shift on $p / 2$. At the third stage, equations (3), (5) and (7) are solved for each individual speckle and the profile of the strain distribution in a composite filled is constructed (Fig. 9).

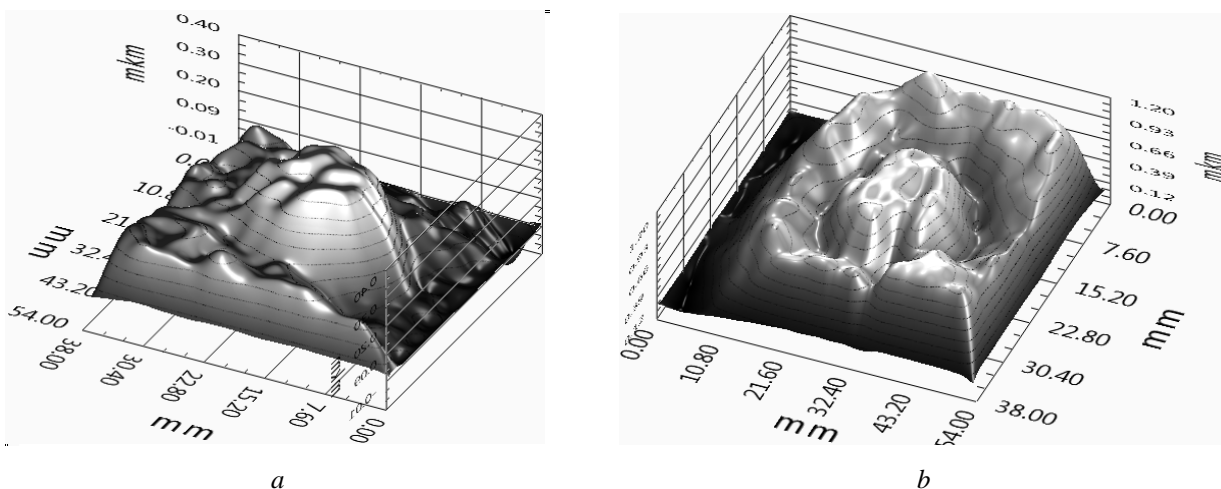


Fig. 9. The profile of the strain distribution in a composite filled with
a – cement; b – epoxy resin of metal reinforcement (Fig. 7)

The strain field of two samples of the composite-cemented (Fig. 9, a) and epoxy resin (Fig. 9, b) of steel reinforcement and heated at 5°C in the center are presented in Fig. 9. For the cement composite (Fig.

9, a), there is an uneven distribution of deformations where the steel reinforcement is protruded from the cement matrix, and a general strain line in the direction of the normal is interrupted in the rear right side of the composite, indicating that there is no adhesion between the metal and the cement. Another picture is observed in Fig. 9, b. There is a good adhesion of the metal to the epoxy resin, but because of the difference in the coefficient of linear thermal expansion, the more flexible matrix material is extruded.

Discussion of the results

The advantage of the proposed method over the known [1–6] is that it allows one to obtain at once a 3-dimensional image of the strain field without an intermediate analysis of the correlation regions of speckles (interference lines). Obviously, the sum of the deformation increments (equation (7)) can reach hundreds of microns, which significantly expands the range of recorded displacements in comparison with known methods, where for large deformations the interference lines become indistinguishable.

In this paper, it is proposed a new approach to increase the speed that increases the speed of the method to the speed of the camera and does not depend on the amplitude-frequency characteristics of the oscillating reference arm of the interferometer. At the calibration stage, after determining the voltage providing a shift to and determining the minimum and maximum intensity of speckles, the specklograms are divided into so-called “representative areas”.

By comparing of two specklograms shifted on $p / 2$, in each representative area a pair of pixels with intensities that corresponds to the phase of the sine and cosine (pixel “sin” and pixel “cos”) is sought. When computing the position of the surface, only two pixels are processed, and the value of the movement is assigned to the entire site. In this case, there is no longer any need to constantly move the support arm, the motion calculation is carried out by one single frame.

This technique somewhat reduces the resolving power of the method, but the performance is increased hundreds of times, which allows us to use high-speed cameras with a frequency of up to 1000 frames per second.

Conclusions

Only one snapshot of the specklogram in the proposed EPSI method can be used in the image processing. This method provides:

- high speed of measurements (up to the CCD camera speed);
- on-line observation of fast dynamic processes;
- obtaining three-dimensional images without analyzing the phase correlation bands;
- high range of measurements (from a few nanometers to hundreds of microns).

References

- [1] Reasons and Methods for Electronic Processing in Coherent Light Systems for Engineering Measurement / J. N. Butters, J. A. Leendertz // Proc. Electro-Opt. Int. – 1971. – Brightox. – England. – P. 189.
- [2] Investigation of Loading Parameters in Detection of Internal Cracks of Composite Material with Digital Shearography / Davood Akbari, Naser Soltani // World Applied Sciences Journal, 2013, 21 (4), pp. 526–535.
- [3] Relation between a linear thermal expansion coefficient and residual stresses / V. Zhukovskiy, A. Gokhman // Technical Physics, 2009, vol. 54, no. 4, pp. 535–541.
- [4] Спосіб швидкісного вимірювання зміни фази об’єктної хвилі методом фазомодульованої спекл-інтерферометрії: пат. 105297 Україна, МПК G 01 B 9/021 (2006.01) / А. Ю. Попов, О. В. Тюрин, О. Я. Бекшаєв., В. Я. Гоцульський; заявник і патентовласник Одеський нац. ун-т ім. І. І. Мечникова. – № а2012 15004; заявл. 27.12.2012; опубл. 25.02.2014, Бюл. № 4. – 4 с.
- [5] Спекл-інтерферометрия / В. П. Рябухо // Соросовский образовательный журнал. – 2001. – № 5. – С. 102–109.
- [6] Method of determining small linear displacement / A. Yu. Popov, W. M. Belous, V. P. Churashev, L. I. Manchenko, V. E. Mandel, Yu. B. A. V. Shugailo, Tyurin // Proceedings of the SPIE, Vol. 3904, p. 291–295 (1999).
- [7] Two approaches to the blind phase shift extraction for two-step electronic speckle pattern interferometry / L. Muravsky, A. Kmet’, T. Voronyak // Optical Engineering, 2013, 52(10), pp. 101909-1–101909-9.